State Concentration Exponent as a Measure of Quickness in Kauffman-type Networks

Shun-ichi Amari[1], Hiroyasu Ando[1], Taro Toyoizumi[1] and Naoki Masuda[2,3]

[1]RIKEN Brain Science Institute, Hirosawa 2-1, Wako, Saitama 351-0198, Japan

[2]Department of Mathematical Informatics, The University of Tokyo, 7-3-1 Hongo, Bunkyo, Tokyo 113-8656, Japan

[3] PRESTO, Japan Science and Technology Agency, 4-1-8 Honcho, Kawaguchi, Saitama 332-0012, Japan

Abstract

The quickness of large network dynamics is quantified by the length of transient paths, an analytically intractable measure. For discrete-time dynamics of networks of binary elements, we address this dilemma with a unified framework termed state concentration, defined as the exponent of the average number of t-step ancestors in state transition graphs. The state transition graph is defined by nodes corresponding to network states and directed links corresponding to transitions. Using this exponent, we interrogate random Boolean and majority vote networks. We find that extremely sparse Boolean networks and majority vote networks with arbitrary density achieve quickness, owing in part to long-tailed indegree distributions. As a corollary, only dense majority vote networks can achieve both quickness and robustness.

I. INTRODUCTION

Networks of binary elements are useful tools for investigating a plethora of dynamical behavior and information processing in biological and social systems. For example, various models of associative memory are used to study neural information processing [1–3]. Random Boolean networks, also known as the Kauffman nets, show rich dynamics and are used to model gene regulation [4–6]. Random majority vote networks are often used to understand mechanisms for ordering in neural information processing [3, 7–9], gene regulation [6], and collective opinion formation in social systems [10].

Properties desirable for dynamics of networks of such binary units include robustness and quickness. A system is defined to be robust when flipping a small number of units' states does not eventually alter behavior of the entire network. For the random Boolean networks, the robustness has been quantified in the context of damage spreading in cellular automata [11–14].

Dynamics are usually called quick if an orbit starting from an arbitrary state reaches the corresponding attractor within a small number of steps on average, i.e., with a short transient length of the dynamics. It is known that the random Boolean networks show long-tailed distributions of the transient length, implying that the transient is long on average [15]. However, analytical evaluation of the transient length is difficult. Therefore, we theoretically study the quickness of dynamics by introducing a new concept of state concentration, extending the previous statistical dynamical framework [7–9]. In particular, the exponent of concentration, which we introduce later, is an analytically tractable quantity to measure the quickness of dynamics in the random Boolean and majority vote networks. Using this exponent, we investigate the compatibility of the robustness and quickness in these two types of networks.

For this purpose, we distinguish densely connected Boolean network (DBN), sparsely connected Boolean network (SBN), densely connected majority vote network (DMN), and sparsely connected majority vote network (SMN). We show that strong state concentration, accompanied by a power law type of the indegree distribution with exponential cutoff, occurs in the majority vote networks (DMN and SMN) but not for the Boolean networks except for extremely sparse cases. Then, we argue that the DMN is the only type among the four types of networks that realizes both robustness and quickness.

II. MODEL

Let us consider a network of n binary units. We define discrete-time dynamics of the network by

$$x_i(t+1) = f_i\left(x_1(t), \ldots, x_n(t)\right) \quad (1 \leq i \leq n), \tag{1}$$

where $x_i(t) \in \{1, -1\}$ is the binary state of the ith unit at time t. For a random Boolean network, each f_i is randomly and independently chosen one of the 2^{2^n} Boolean functions on the n units. For a majority vote network,

$$f_i(x_1, \ldots, x_n) = \mathrm{sgn}\left(\sum_{j=1}^{n} w_{ij} x_j\right) \ (1 \leq i \leq n), \tag{2}$$

where sgn indicates the sign function. We consider an ensemble of randomly generated majority vote networks where w_{ij} are independently and identically distributed Gaussian random variables. In general, a constant or random threshold could be included in the above dynamical expression, which we omit here for simplicity. If the value of $f_i\left(x_1, \ldots, x_n\right)$ depends only on randomly chosen K units for each i, the model is called the K-sparse network [4, 5]. The DBN and DMN correspond to $K \propto n$, and the SBN and SMN correspond to $K \ll n$. We study typical dynamical behavior of the random DBN, SBN, DMN, and SMN.

III. DISTANCE LAW IN STATE TRANSITION

The network state at time t is given in vector form as

$$\boldsymbol{x}(t) = \left(x_1(t), \ldots, x_n(t)\right). \tag{3}$$

Let $X = \{\boldsymbol{x}\}$ be the set of the $N \equiv 2^n$ states. Given a network, the state transition is a mapping from X to itself. We write it briefly as $\boldsymbol{x}(t+1) = f\boldsymbol{x}(t)$.

The dynamics of the distance between two state trajectories has been studied to characterize dynamics in these networks. We define the normalized Hamming distance between two states $\boldsymbol{x}$ and $\boldsymbol{y}$ in X by

$$D(\boldsymbol{x}, \boldsymbol{y}) = \frac{1}{2n} \sum_{i=1}^{n} \left|x_i - y_i\right|. \tag{4}$$

It should be noted that the distance is restricted to the range $0 \leq D(\boldsymbol{x}, \boldsymbol{y}) \leq 1$. If $d' = \varphi(d)$ holds true for a function $\varphi(d)$ for any $\boldsymbol{x}$ and $\boldsymbol{y}$ almost always as $n \to \infty$, where $d = D(\boldsymbol{x}, \boldsymbol{y})$ and $d' = D(f\boldsymbol{x}, f\boldsymbol{y})$, we call it the distance law. For the DBN, $\varphi(d) = 0$ $(d = 0)$ and $\varphi(d) = 1/2$ $(d \neq 0)$. For the SBN [16],

$$\varphi(d) = (1/2)\left[1 - (1-d)^K\right]. \tag{5}$$

For the DMN [7–9],

$$\varphi(d) = (2/\pi)\sin^{-1}\sqrt{d}. \tag{6}$$

For the SMN [17],

$$\varphi(d) = \sum_{j=0}^{K} g_{K,j} \binom{K}{j} d^j (1-d)^{K-j}, \tag{7}$$

where $\binom{K}{j}$ is the binomial coefficient and

$$g_{K,j} = (2/\pi)\sin^{-1}\sqrt{j/K}. \tag{8}$$

The dynamics of the distance under annealed approximation are given by $d_{t+1} = \varphi(d_t)$ [7, 16–18]. For all the four types of networks, $\varphi(0) = 0$. For the DBN, $\varphi(d)$ is discontinuous at $d = 0$, and the dynamics are essentially the same as those of the random mapping on the N states. Therefore, various properties of dynamics such as the number of attractors, transient length, and cycle period are well characterized [4, 5, 7]. For the SBN, DMN, and SMN, $\varphi(d)$ is continuous at $d = 0$. It is known that $d = 0$ is a stable fixed point of mapping φ (i.e., $0 < \varphi(0)' < 1$) only for the SBN and SMN with $K = 1$ or 2. Otherwise, d_t converges to a positive value $\overline{d}$ satisfying $\overline{d} = \varphi\left(\overline{d}\right)$. The convergence of the distance is usually fast and happens after ~ 10 steps except for DBN where one step is enough for the distance to converge.

IV. EXPONENT OF STATE CONCENTRATION

The transient length before the orbit enters the attractor is analytically intractable. To quantify the quickness of the dynamics by using an alternative order parameter called the exponent of state concentration, we use the so-called state transition graph [4, 5, 19] defined as follows. A map f, either Boolean or majority vote, induces a graph on N nodes. Each state $\boldsymbol{x} \in X$ defines a node and has exactly one outgoing link directed to node $f\boldsymbol{x}$.

Suppose that each of the $N = 2^n$ nodes (i.e., states) has a token at $t = 0$. For each $t(\geq 0)$, an application of f moves all the tokens at each node $\boldsymbol{x}$ to node $f\boldsymbol{x}$. Repeated applications of mapping f elicit concentration of tokens at specific nodes. We denote by $f^{-t}\boldsymbol{x}$ the set of nodes whose tokens move to $\boldsymbol{x}$ after t steps and by $|f^{-t}\boldsymbol{x}|$ the number of tokens at node $\boldsymbol{x}$ after t steps. Tokens are initially equally distributed, i.e., $|f^0\boldsymbol{x}| = 1$ for each $\boldsymbol{x}$, and the total number of tokens is conserved, i.e.,

$$\sum_{\boldsymbol{x}\in X} \left|f^{-t}\boldsymbol{x}\right| = N \tag{9}$$

for $t \geq 0$.

The indegree of node $\boldsymbol{x}$ in the state transition graph is equal to $|f^{-1}\boldsymbol{x}|$. The nodes with $f^{-1}\boldsymbol{x} = \emptyset$, where $\emptyset$ is the empty set, do not have parent nodes. The set of such nodes is called the garden of Eden [4]. and denoted by E_1. The nodes $\boldsymbol{x} \in E_1$ only appear as initial state. Only the nodes $\boldsymbol{x} \in X - E_1$ receive tokens at $t = 1$. In general, we define $E_t \equiv \{\boldsymbol{x} \mid f^{-t}\boldsymbol{x} = \emptyset\}$, i.e., the set of nodes that do not own tokens at time step t. There exists integer T such that

$$\phi \subset E_1 \subset E_2 \subset \cdots \subset E_T = E_{T+1} = \cdots \equiv E^*, \tag{10}$$

where T is the longest transient period and E^* is the set of the transient states. The set of the attractors is given by $A = X - E^*$ (Fig. 1).

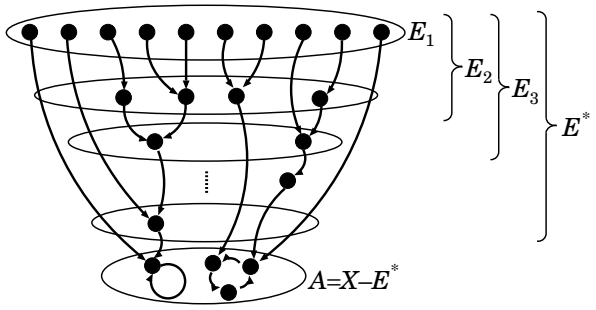

FIG. 1: Schematic of dynamics of state concentration. E_1 indicates the garden of Eden, E_2 indicates the nodes that do not have grandparents, and A indicates the set of attractors.

To quantify the state concentration, we consider the frequency with which a randomly selected token at $\boldsymbol{x}(0)$ and $t = 0$ meets other tokens after applying f. We write the relationship $f\boldsymbol{x}(0) = \boldsymbol{x}(1)$ succinctly as $\boldsymbol{x}(0) \to \boldsymbol{x}(1)$. Let $\overline{S}_1$ be the conditional expectation

$E\left[|f^{-1}\boldsymbol{x}(1)| \mid \boldsymbol{x}(0) \to \boldsymbol{x}(1)\right]$ of the indegree of node $\boldsymbol{x}(1)$ given that $\boldsymbol{x}(0) \to \boldsymbol{x}(1)$ and that $\boldsymbol{x}(0)$ is selected with equal probability (i.e., $1/N$). In general, we denote by $\overline{S}_t$ the expected number of t-fold parent nodes of a node $\boldsymbol{x}(t)$ conditioned by a state transition path ending at $\boldsymbol{x}(t)$ through which a token has traveled, i.e.,

$$\overline{S}_t \equiv E\left[\left|f^{-t}\boldsymbol{x}(t)\right| \mid \boldsymbol{x}(0) \to \cdots \to \boldsymbol{x}(t-1) \to \boldsymbol{x}(t)\right]. \tag{11}$$

Obviously $\overline{S}_0 = 1$ and sequence $\{\overline{S}_t\}$ is monotonically nondecreasing in t. If

$$\overline{S}_t = e^{c_t n},\ c_t > 0, \tag{12}$$

holds true for large n, the tokens are exponentially concentrated on nodes having at least a t-fold parent node. We refer to

$$c_t = \lim_{n\to\infty} \frac{\log \overline{S}_t}{n} \tag{13}$$

as t-step exponent of concentration. Exponent c_t provides an n-independent measure of state concentration without explicitly evaluating the statistics of the transient.

The stochastic symmetry of units makes the calculation of $\overline{S}_t$ tractable. To explain the symmetry, we consider the majority vote network; similar arguments hold true for the Boolean network. Because weights w_{ij} are independently and identically distributed, the probability distribution of mapping f is invariant under permutation of $x_1, \ldots, x_n$, which are passed as the arguments to f_i $(1 \le i \le n)$. In addition, the probability is invariant under the flip of sign of each x_i. Therefore, the following gauge invariance holds. First, the probability distribution of $\boldsymbol{x}(t)$ is invariant under permutation of the unit indices. Second, the probability distribution is invariant under the sign flip of any $x_i(t)$. Because any state is mapped in a single step to a given $\boldsymbol{x}$ by permutation and sign flip, all the states are stochastically equivalent. Therefore, $\mathrm{Prob}\{|f^{-1}\boldsymbol{x}| = k\}$, for example, is the same for all $\boldsymbol{x}$, and $\mathrm{Prob}\{\boldsymbol{x}(0) \to \boldsymbol{x}(1)\} = 1/N$ for any $\boldsymbol{x}(0)$ and $\boldsymbol{x}(1)$.

We define

$$r_k = \mathrm{Prob}\left\{\left|f^{-1}\boldsymbol{x}(1)\right| = k \ \mid \boldsymbol{x}(0) \to \boldsymbol{x}(1)\right\}, \tag{14}$$

i.e., the indegree distribution of node $\boldsymbol{x}(1)$ conditioned by $\boldsymbol{x}(0) \to \boldsymbol{x}(1)$. The symmetry guarantees that r_k is independent of $\boldsymbol{x}(0)$ and $\boldsymbol{x}(1)$. Let us compute

$$\overline{S}_1 = \sum_{k=1}^{N} k r_k. \tag{15}$$

We denote by $\boldsymbol{y}(0)$ a node such that $D\left(\boldsymbol{x}(0), \boldsymbol{y}(0)\right) = d$ for a given $\boldsymbol{x}(0)$. The number of nodes with distance d away from $\boldsymbol{x}(0)$ is given by

$$\binom{n}{nd} \approx e^{nH(d)}, \tag{16}$$

where

$$H(d) \equiv -d \log d - (1-d) \log(1-d) \tag{17}$$

is the entropy. The probability that $D\left(f\boldsymbol{x}(0), f\boldsymbol{y}(0)\right) = d'$ (see Fig. 2 for a schematic illustration of this situation) is given by

$$\psi\left(d' \mid d\right) \equiv \binom{n}{nd'} \varphi(d)^{nd'} \left[1-\varphi(d)\right]^{n(1-d')}. \tag{18}$$

In particular,

$$\psi(0 \mid d) = \left[1-\varphi(d)\right]^n = \mathrm{Prob}\left\{f\boldsymbol{y}(0) = \boldsymbol{x}(1) \mid \boldsymbol{x}(0) \to \boldsymbol{x}(1)\right\}. \tag{19}$$

By using the saddle-point approximation, we obtain

$$\begin{aligned} \overline{S}_1 &= \sum_{nd=0}^{n} \binom{n}{nd} \psi(0 \mid d) \\ &\approx \int \exp n \left\{H(z) + \log\left[1-\varphi(z)\right]\right\} dz \propto e^{nc_1}, \end{aligned} \tag{20}$$

where

$$c_1 = H\left(d^*\right) + \log\left[1-\varphi\left(d^*\right)\right] \tag{21}$$

and

$$d^* = \arg\max_d \left\{H(d) + \log\left[1-\varphi(d)\right]\right\}. \tag{22}$$

To evaluate c_t in general, we consider a t-step state transition path $X_t = \{\boldsymbol{x}(0) \to \boldsymbol{x}(1) \to \cdots \to \boldsymbol{x}(t) = \boldsymbol{x}^*\}$ ending at $\boldsymbol{x}^*$ and calculate the conditional probability that another path $Y_t = \{\boldsymbol{y}(0) \to \cdots \to \boldsymbol{y}(t)\}$ ends at the same $\boldsymbol{x}^*$. $\overline{S}_t$ is the expectation of the number of such t-step paths. Let us denote the distance $D(\boldsymbol{x}(t'), \boldsymbol{y}(t'))$ by $d_{t'}$, where $0 \le t' \le t$ and $d_t = 0$. Then, under the Markov assumption, the probability of path Y_t conditioned by path X_t is represented in terms of the distances of the two sequences, i.e., $d_{t'}, 0 \le t' \le t$, by

$$\mathrm{Prob}\{Y_t \mid X_t\} = \prod_{t'=1}^{t'=t} \psi(d_{t'} \mid d_{t'-1}). \tag{23}$$

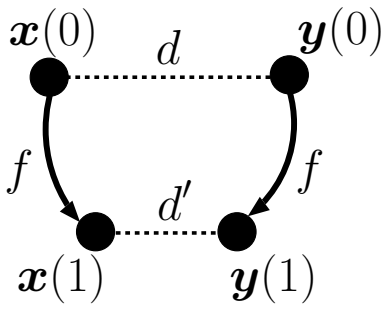

FIG. 2: Schematic of one-step dynamics of the distance.

The Markov assumption is valid for large n and a finite t. Because there are $\binom{n}{nd_0}$ states $\boldsymbol{y}(0)$ possessing distance d_0 from $\boldsymbol{x}(0)$, the expected number of paths is given by the integration of $\binom{n}{nd_0}$ Prob $\{Y_t \mid X_t\}$ over all the possible distance sequences $\{d_0, \ldots, d_{t-1}, d_t = 0\}$. By using the saddle-point approximation, we have

$$\overline{S}_t = \exp\left[nH(d_0^*) + \sum_{t'=1}^{t} \log \psi(d_{t'}^* \mid d_{t'-1}^*)\right] \tag{24}$$

for large n, where $d_{t'}^*$ are the maximizers of the integrand in the path integration. Equation (24) implies

$$\begin{aligned} c_t = &\sum_{t'=1}^{t} \left\{ H(d_{t'-1}^*) + d_{t'}^* \log \varphi(d_{t'-1}^*) \right. \\ &\left. + (1 - d_{t'}^*) \log \left[1 - \varphi(d_{t'-1}^*)\right] \right\}. \end{aligned} \tag{25}$$

For example, for $t = 2$, we obtain

$$\begin{aligned} c_2 = &H(d_0^*) + H(d_1^*) + \log\left[1 - \varphi\left(d_1^*\right)\right] + d_1^* \log \varphi\left(d_0^*\right) \\ &+ (1 - d_1^*) \log\left[1 - \varphi\left(d_0^*\right)\right], \end{aligned} \tag{26}$$

where

$$\begin{aligned} \{d_0^*, d_1^*\} = &\arg\max_{d_0, d_1} \left\{ H(d_0) + H(d_1) + \log\left[1 - \varphi\left(d_1\right)\right] \right. \\ &\left. + d_1 \log \varphi\left(d_0\right) + (1 - d_1) \log\left[1 - \varphi\left(d_0\right)\right] \right\}. \end{aligned} \tag{27}$$

On the basis of the expression of φ for the SBN and SMN shown before, the dependence of c_1, c_2, c_3, and c_4 on K is plotted in Fig. 3. For the SBN, c_t $(1 \leq t \leq 4)$ converges to 0

quickly as K increases. For the DBN, which is the case for $K = n$, we trivially obtain $c_t = 0$ at least for small t because f is equivalent to the random mapping. Figure 3 indicates that the state concentration occurs only for very small K in the random Boolean network. In contrast, the state concentration occurs even for large K in the majority vote network. In particular, for the DMN with $K \to n$, we obtain $c_1 \approx 0.157$ [9]. Figure 3 also indicates that the state concentration quickly proceeds as t increases, except in the DBN.

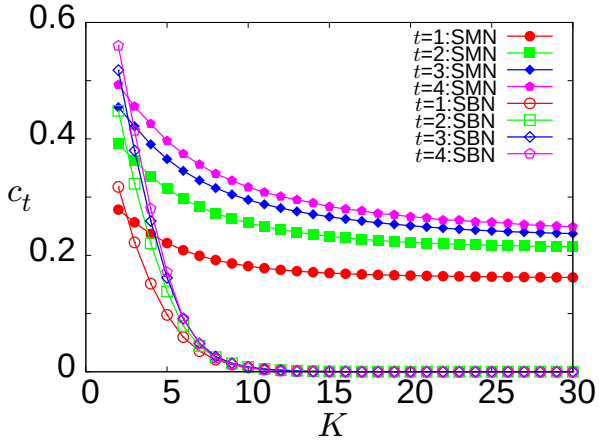

FIG. 3: (Color online) c_1, c_2, c_3, and c_4 for the SMN and SBN.

We verified Eq. (13) by comparing $\overline{S}_t$ obtained from direct numerical simulations (i.e., Eq. (11)) and c_t generally given by Eq. (25). The results shown in Fig. 4 indicate that the theory (lines) seems to agree with numerical results at least for large N; although the largest N value shown in the figure is only $n = 25$. Therefore, the Markov assumption (Eq. (23)), also implicitly assumed for $t = 2$, 3, and 4 in Fig. 3, roughly holds true up to $t \approx 4$ for large n.

Theoretically, most sequences Y_t that meet X_t after t steps of state transition own the sequence of distance given by $\boldsymbol{d}_t^* = \left\{d_0^*, d_1^*, \cdots, d_{t-1}^*, d_t^* = 0\right\}$. In particular, a majority of the initial states Y_0 is initially separated from X_0 by $d_0^*(t)$. Figure 4 suggests that this is the case at least up to $t \approx 4$ for large n. The sequence of distance $\boldsymbol{d}_t^*$ is shown for $1 \leq t \leq 4$ in Fig. 5.

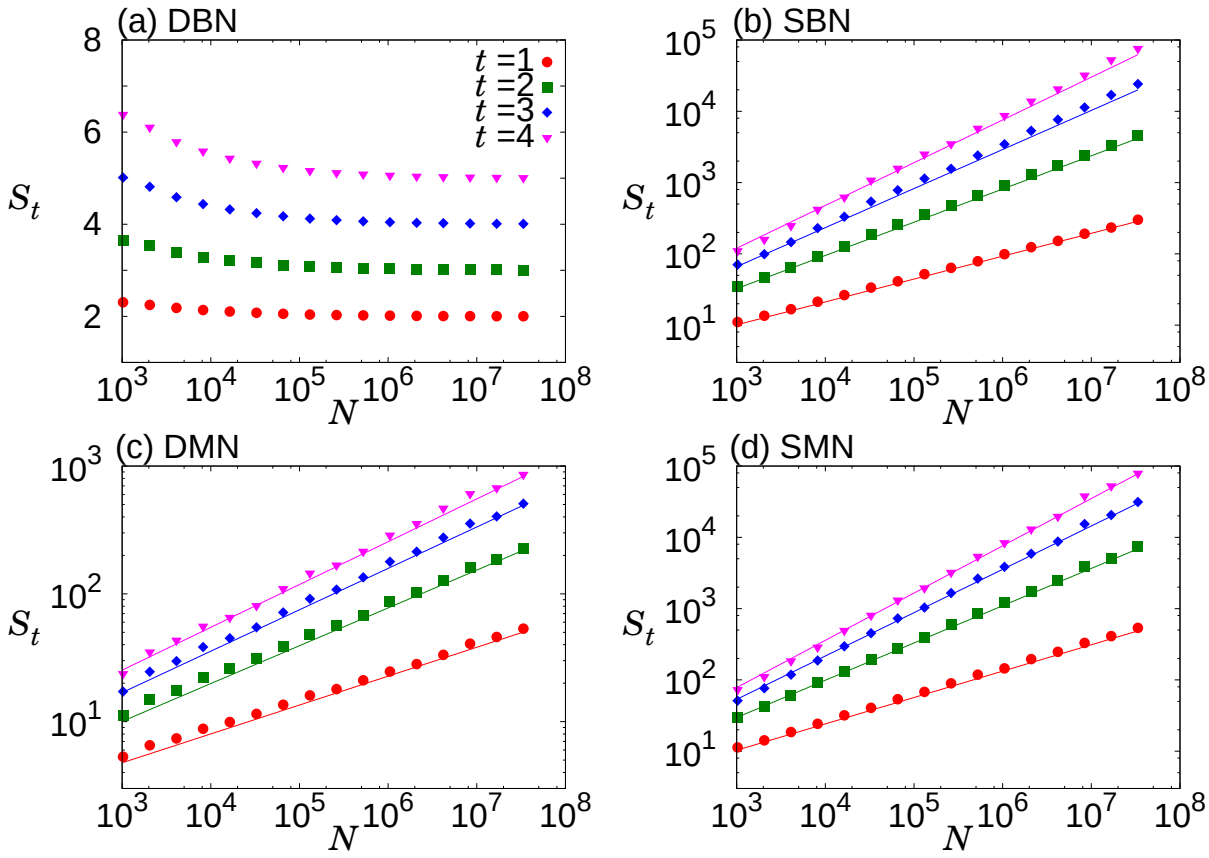

FIG. 4: (Color online) $\overline{S}_t$ exponentially increases with n except in the DMN. (a) DBN, (b) SBN with $K = 3$, (c) DMN, and (d) SMN with $K = 3$. The lines in (b) indicate the theoretical estimates, i.e., $\overline{S}_1 \propto N^{0.321}$, $\overline{S}_2 \propto N^{0.466}$, $\overline{S}_3 \propto N^{0.548}$, and $\overline{S}_4 \propto N^{0.600}$. Similarly, the lines in (c) indicate $\overline{S}_1 \propto N^{0.226}$, $\overline{S}_2 \propto N^{0.296}$, $\overline{S}_3 \propto N^{0.324}$, and $\overline{S}_4 \propto N^{0.335}$. The lines in (d) indicate $\overline{S}_1 \propto N^{0.370}$, $\overline{S}_2 \propto N^{0.523}$, $\overline{S}_3 \propto N^{0.608}$, and $\overline{S}_4 \propto N^{0.663}$. Each point in the figure represents the average of $\overline{S}_t$ over 10^3 realizations of the network.

V. INDEGREE DISTRIBUTION OF THE STATE TRANSITION GRAPH

We calculate the incoming degree distribution

$$p_k = \text{Prob}\left\{\left|f^{-1}\boldsymbol{x}\right| = k\right\}, \tag{28}$$

where k is the indegree of a state and $\sum_{k=0}^{N} p_k = 1$. Because each node in the state transition graph has exactly one outgoing link, we have

$$\langle k\rangle = \sum_{k=0}^{N} k p_k = 1, \tag{29}$$

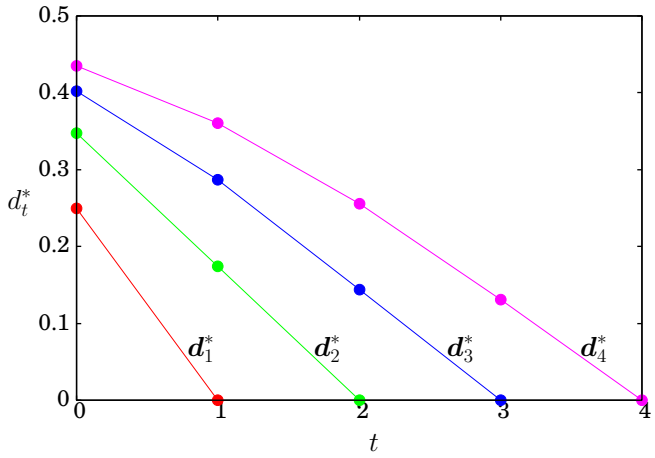

FIG. 5: (Color online) Sequence of the most likely distances $\boldsymbol{d}_t^* = \left\{d_0^*, d_1^*, \cdots, d_{t-1}^*, d_t^* = 0\right\}$ for $1 \leq t \leq 4$.

where $\langle\cdot\rangle$ indicates the expectation. Because $r_k = kp_k$ [7] (also see [20] for an example), we obtain

$$\left\langle k^2 \right\rangle = \sum_{k=0}^{N} k^2 p_k = \sum_{k=0}^{N} k r_k = \overline{S}_1 = e^{nc_1}. \tag{30}$$

Therefore, $c_1 > 0$ indicates that $\langle k^2 \rangle$ diverges in the limit of $N = 2^n \to \infty$, reminiscent of the scale-free property of the state transition graph [20–22].

For the DBN, the state transition graph is the directed random graph in which p_k obeys the Poisson distribution (i.e., $p_k = 1/ek!$) with mean and variance 1 [4, 5]. Therefore, $\langle k^2 \rangle = 2$, proving that $c_1 = 0$ for the DBN (i.e., no exponential state concentration). This is consistent with Fig. 4(a) (circles). Figure 3 suggests that $c_1 \approx 0$ when K is approximately larger than 10. Therefore, the degree distribution of the state transition graph is also narrowly distributed for the SBN with $K \geq 10$. We verified that the numerically obtained indegree distribution for the random Boolean network with $n = 30$ and $K = 20$ approximately obeys the Poisson distribution (Fig. 6(a)).

In contrast, a positive value of c_1 found for the SBN with small K, DMN, and SMN (Fig. 3) indicates that $\langle k^2 \rangle \, (= \overline{S}_1)$ diverges exponentially in n. This is actually the case, as shown in Fig. 4(b, c, d). For scale-free networks with $p_k \approx k^{-\gamma}$, the extremal criterion would lead to $\gamma \approx (c_1 + 3\log 2)/(c_1 + \log 2)$ [21, 22]. However, the degree distribution numerically obtained for the DMN, shown in Fig. 6(b), deviates from a power law. The degree distribution numerically obtained for the SBN is also different from a power law [19].

To guides to the eyes, a fitting curve on the basis of a power law with an exponential cutoff is shown by the line in Fig. 6(b). In fact, the power law is not the only distribution that yields the divergence of $\langle k^2 \rangle$. In the present case, the position of the exponential cutoff may mildly diverge as N becomes large.

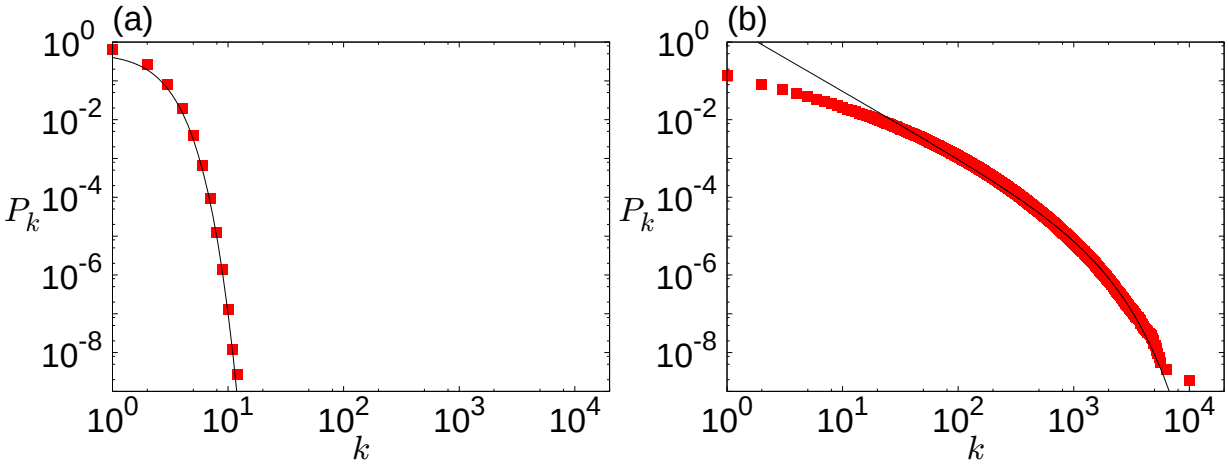

FIG. 6: (Color online) Complementary indegree distribution of p_k (i.e., $P_k \equiv \sum_{k'=k}^{N} p_{k'}$) of the state transition graph. (a) Random Boolean network with $n = 30$ and $K = 20$. The numerical results are shown by squares, and the Poisson distribution with mean 1 is indicated by the line. (b) Random majority vote network with $n = 30$ and $K = 30$. A fitting curve, $P_k \propto k^{-1.72} \exp\{-0.001k\}$, obtained from the least square error method, is shown by the line as guides to the eyes.

VI. DISCUSSION AND CONCLUSIONS

In summary, we provided a unified framework for analyzing the state concentration. We found that the state concentration occurs in the SBN with small K, DMN, and SMN, but not in the DBN. We also revealed the long-tailed distributions of the indegree of the state transition graph in the SBN, DMN, and SMN, but not in the DBN.

We briefly discuss the relationship between the quickness, measured by the exponent of state concentration in this study, and the robustness of the dynamics. The robustness of the dynamics is often measured in terms of damage spreading. It is a long-term property concerning the stability of $d = 0$ for mapping φ. As we mentioned, $d = 0$ is an unstable fixed point of φ unless $K = 1$ or 2. Although the SMN with $K = 1$ or 2 satisfies quickness and robustness, we do not discuss these cases because the dynamics in these cases are just frozen

[17, 18]. Here we consider a simpler measure of robustness based on a one-step property, i.e., how a difference by a single bit evolves after a single application of f. This is essentially the same as the Boolean derivative, a measure of the robustness used for analyzing random Boolean networks [11–14]. In the SMN, the probability that a single bit flip results in a single bit flip after the application of f is given by

$$g_{K,1} = (2/\pi) \sin^{-1} \sqrt{1/K}. \tag{31}$$

Because $g_{K,1}$ is equal to 0.5 for $K = 2$ and decreases according to $\approx 2/(\pi\sqrt{K})$ as K increases, the random majority vote network is robust except for very small K. However, in the random Boolean network, the same flip probability is equal to $1/2 - 1/2^{2^K}$, which quickly approaches $1/2$ as K increases. In particular, the flip probability for the Boolean network at $K = 2$ is equal to $7/16 = 0.4375$, which is close to those for the majority vote network with $K = 2$ (i.e., 0.5) and $K = 3$ (i.e., 0.392). Although the Boolean network with $K = 1$ has sufficient robustness, the dynamics in this case are frozen [23]. Therefore, we regard that the robustness of the one-step dynamics holds true in the DMN, but not in the DBN, SBN, and SMN. By combining this observation with our main results, we regard that quickness and robustness suitably compromise in the DMN, but not in the DBN, SBN, and SMN.

---

[1] S. -I. Amari, IEEE Trans. Computers, **11**, 1197 (1972).

[2] J. J. Hopfield, Proc. Natl. Acad. Sci. USA, **79**, 2554 (1982).

[3] J. Hertz, A. Krogh, and R. G. Palmer, Introduction to the theory of neural computation, Westview Press (1991).

[4] S. A. Kauffman, Physica D, **10**, 145 (1984).

[5] S. A. Kauffman, The Origin of Orders: Self-Organization and Selection in Evolution, Oxford Univ Press (1993).

[6] S. Bornholdt, J. Roy. Soc., Interface, **5**, 85 (2008).

[7] S. Amari, Kybernetik, **14**, 201 (1974).

[8] S. Amari, K. Yoshida, and K. Kanatani, SIAM J. Appl. Math., **33**, 95 (1977).

[9] S. Amari, Proc. IEEE, **78**, 1443 (1990).

[10] C. Castellano, S. Fortunato, and V. Loreto, Rev. Mod. Phys., **81**, 591 (2009).

[11] B. Luque and R. V. Solé, Phys. Rev. E, **55**, 257 (1997).

[12] B. Luque and R. V. Solé, Physica A, **284**, 33 (2000).

[13] S. Kauffman, C. Peterson, B. Samuelsson, and C. Troein, PNAS, **101**, 17102 (2004).

[14] I. Shmulevich and S. Kauffman, Phys. Rev. Lett., **93**, 048701 (2004).

[15] A. Bhattacharjya and S. Liang, Phys. Rev. Lett., **77**, 1644 (1996).

[16] B. Derrida and Y. Pomeau, Europhysics. Lett., **1**, 45 (1986); B. Derrida and G. Weisbuch, J. Physique (Paris), **47**, 1297 (1986).

[17] B. Derrida, J. Phys. A, **20**, L721 (1987).

[18] K. E. Kürten, Phys. Lett. A, **129**, 157 (1988); K. E. Kürten, J. Phys. A, **21**, L615 (1988).

[19] A. Shreim, A. Berdahl, V. Sood, P. Grassberger, and M. Paczuski, New J. Phys., **10**, 013028 (2008).

[20] M. E. J. Newman, S. H. Strogatz, and D. J. Watts, Phys. Rev. E, **64**, 026118 (2001).

[21] M. E. J. Newman, Contem. Phys., **46**, 323 (2005).

[22] S. N. Dorogovtsev, A. V. Goltsev, and J. F. F. Mendes, Rev. Mod. Phys., **80**, 1275 (2008).

[23] H. Flyvbjerg and N. J. Kjaer, J. Phys. A, **21**, 1695 (1988).